End of Performance Prediction of Lithium-ion Batteries

YI-FU WANG[a], SHENG-TSAING TSENG[b*], BO HENRY LINDQVIST[c], KWOK-LEUNG TSUI[d]

[a] National Chung Cheng University, Chiayi, Taiwan.

[b] National Tsing Hua University, Hsinchu, Taiwan.

[c] Norwegian University of Science and Technology, Trondheim, Norway.

[d] City University of Hong Kong, Kowloon, Hong Kong.

Abstract

Rechargeable batteries are critical components for the performance of portable electronics and electric vehicles. The long term health performance of rechargeable batteries is characterized by state of health which can be quantified by end of performance (EOP) and remaining useful performance. Focusing on EOP prediction, this paper first proposes an accelerated testing version of the trend-renewal process model to address this decision problem. The proposed model is also applied to a real case study. Finally, a NASA dataset is used to address the prediction performance of the proposed model. Comparing with the existing prediction methods and time series models, our proposed procedure has better performance in the EOP prediction.

Key Words: Accelerated Trend-Renewal Process, EOP, Recurrent Events.

*corresponding author

Dr. Wang is an Assistant Professor at the Department of Mathematics, National Chung Cheng University. His email address is ifwang027@gmail.com.

Dr. Tseng is a Professor at the Institute of Statistics, National Tsing Hua University. His email address is sttseng@stat.nthu.edu.tw.

Dr. Lindqvist is a Professor at the Department of Mathematical Sciences, Norwegian University of Science and Technology. His email address is bo.lindqvist@ntnu.no.

Dr. Tsui is a Professor at the Department of Systems Engineering and Engineering Management, City University of Hong Kong. His email address is kltsui@cityu.edu.hk.

1 Introduction

Rechargeable batteries are critical components for the performance of portable electronics and electric vehicles. The long term health performance of rechargeable batteries is characterized by a key parameter called state of health (SOH). SOH denotes the remaining performance of a battery over its whole life cycle, which is quantified by end of performance (EOP) and remaining useful performance (RUP). This paper investigates the modeling of accelerated testing and prediction of EOP for lithium rechargeable batteries.

1.1 EOP Prediction of Battery Performance

Battery capacity is a most common index to describe the battery performance. Technically, EOP of battery is defined as the cycle time when the capacity ratio (the ratio of the discharge capacity of battery to its rated capacity, CR) is reduced to a specific threshold and it is considered to be failed if its CR reaches this threshold, which is usually defined at 80% (Spotnitz (2003), Saha *et al.* (2007)). Moreover, RUP is defined as the duration between current time and EOP.

A review of lithium-ion battery prognostics and health management (PHM) were given

in Zhang and Lee (2011). Nowadays, there are two common approaches for battery PHM: physics-of-failure (PoF) models and data-driven approaches. PoF models take into account the knowledge of a battery's life cycle loading conditions, geometry, material properties, and failure mechanisms to estimate its RUP and/or EOP (Gu *et al.* (2007), Pecht and Dasgupta (1995), He *et al.* (2011)). Although PoF models are accurate, they are not appropriate to online applications due to size limitations, high cost, high requirement for computation and strict environmental variables (Xing *et al.*, 2013).

In contrast, data-driven approaches do not require any knowledge of failure mechanisms, they estimate the RUP and/or EOP only relying on the capacity data. He *et al.* (2011) developed an exponential model consisting of two exponential functions to capture the battery capacity fade. Micea *et al.* (2011) proposed an empirical second-order polynomial model to predict the capacity function. Pattipati *et al.* (2011) used the support vector regression (SVR) to estimate the RUP. Xing *et al.* (2013) proposed an ensemble model by combining exponential and polynomial regression models to predict the RUP based on particle filtering. Other research for EOP and/or RUP prediction can be found in Long *et al.* (2013), Miao *et al.* (2013), Tang *et al.* (2014), Lu *et al.* (2014), Cheng *et al.* (2015), and Xu *et al.* (2016).

Nowadays, the product's lifetime may be extensive. Under this situation, accelerated life testing is an efficient way to shorten the life-testing time, since environmental conditions have a big impact on the battery degradation. However, most existing data-driven models were constructed under a specific discharge rate or a fixed temperature to implement the EOP and/or RUP prediction. For the purpose of improving the experiment efficiency, it is important to develop an accelerated testing model for capturing the battery degradation

under more severe environment conditions such as higher discharge rates or temperatures. Ng *et al.* (2014) studied a naive Bayes model for RUP prediction of batteries under different operating conditions and ambient temperatures by formulating a data-driven classification method (the naive Bayes classification). In this paper, we will develop a model to capture the battery capacity function under the accelerated testing, and further obtain the EOP and/or RUP based on extrapolated prediction on use condition. In the following, we propose a repairable system model to characterize the battery degradation under accelerated testing.

1.2 The Trend-Renewal Process

The trend-renewal process (TRP) is originally designed to be a model for failure events of repairable systems, first presented in Lindqvist *et al.* (2003). It is by definition a time-transformed renewal process. The time transformation is the cumulative version of a so-called trend function, $\lambda(t)$, similar to the intensity function of a non-homogeneous Poisson process (NHPP), while the (latent) renewal process (RP) is characterized by the inter-arrival distribution, F, called the renewal distribution of the TRP. In some sense the TRP is constructed as the "least common multiple" of the NHPP and the RP. The advantage of using a TRP instead of an RP is its ability to represent a possible trend in the inter-failure times. This makes the TRP a powerful tool, despite its simple structure.

The present paper is concerned with the fitting of TRP models to cycle times of a rechargeable battery. Typically, these cycle times will be (stochastically) decreasing with time, making the i.i.d. assumption of an RP inappropriate. On the other hand, the addition of a trend function, as is exactly what is done in the TRP, will enable the modeling of such

a decrease.

Until now, the TRP has mostly been used to model events occurring in time, see, Lindqvist *et al.* (2003), Cook and Lawless (2007, Ch. 5.2), Jokiel-Rokita and Magiera (2012), and Franz *et al.* (2014), for examples. An interesting application to occurrence of earthquakes is found in Bebbington (2010). The precise mathematical definition of the TRP is given in Section 3, where also a heterogeneous version based on observation of several processes under different stresses is considered.

The rest of this article is organized as follows. Section 2 considers a real example to motivate the study. Section 3 develops a preliminary analysis for this motivated example by using TRP model. Section 4 introduces the problem formulation of an accelerated testing version of TRP (and hereafter denoted by ATRP) model and the corresponding statistical inference, including a method for the EOP prediction. Section 5 applies the proposed procedure to analyse the battery example stated in Section 2. Section 6 uses two examples to compare the prediction performances between the proposed ATRP model and some existing models (including linear regression with time series errors model). Section 7 gives another version of ATRP model. Finally, some concluding remarks are addressed in Section 8.

2 Motivating Example

In the following experiment, we have 9 lithium-ion batteries which are tested under the charge and discharge processes. During the charging process, all samples are fully charged at a constant current of 1C rate (where 1C is defined as a current that will discharge the rated capacity of the battery in 1 hour); while in the discharging process, three discharge

rates (1C, 3C, 5C) are adopted to shorten the life testing time. Note that the normal use condition for the discharge rate is 0.5C. (In Section 6, the information of extra batteries under normal use will be used for the purpose of model validation). For each discharge rate, we have 3 batteries and their CRs were recorded up to 520 cycle times. Figure 1 shows the plots of CRs of these samples. The plots demonstrate that CR increases in the beginning and then decreases gradually. This is a common phenomenon in a rechargeable battery. In our study, the first stage with 70 cycle times is omitted for analysis as it is not so helpful on predicting EOP. Therefore, we trim the observations into 450 (=520-70) cycle times. In addition, from the plot, it is seen that one degradation path (which is highlighted with red color) in 5C is completely different from that of the other two batteries. This behavior may be due to either an outlier sample or incorrect calibration of metrology equipment. Hence, we delete this sample in the following analysis.

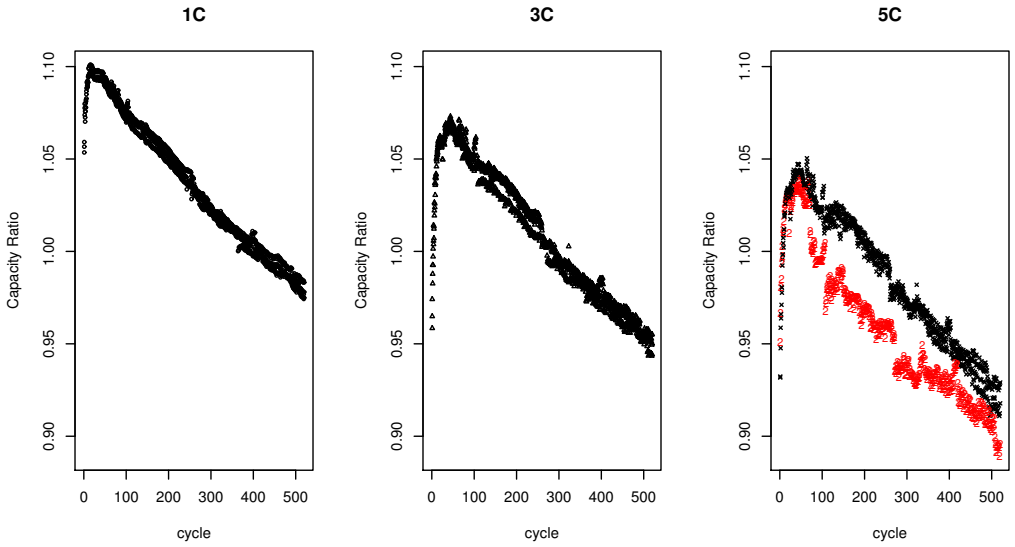

Figure 1: The CR plots under three discharge rates.

To simplify our problem, we put 10 cycle times into a group and simply call it a g-cycle time. In addition, we define CR_g as the summation of 10 capacity ratios in a group. The CR_g plots of 8 samples with respect to g-cycle time are shown in Figure 2. The plot demonstrates that CR_g and g-cycle have a very high linear relationship. Therefore, we may consider to adopt a linear regression model to extrapolate the EOP performance under use condition 0.5C. However, battery data are typically time-dependent (time series) data. The i.i.d. assumption in the error term of regression model is hence not valid. We will further address this issue via linear regression model with a time series error later in Section 6.1.

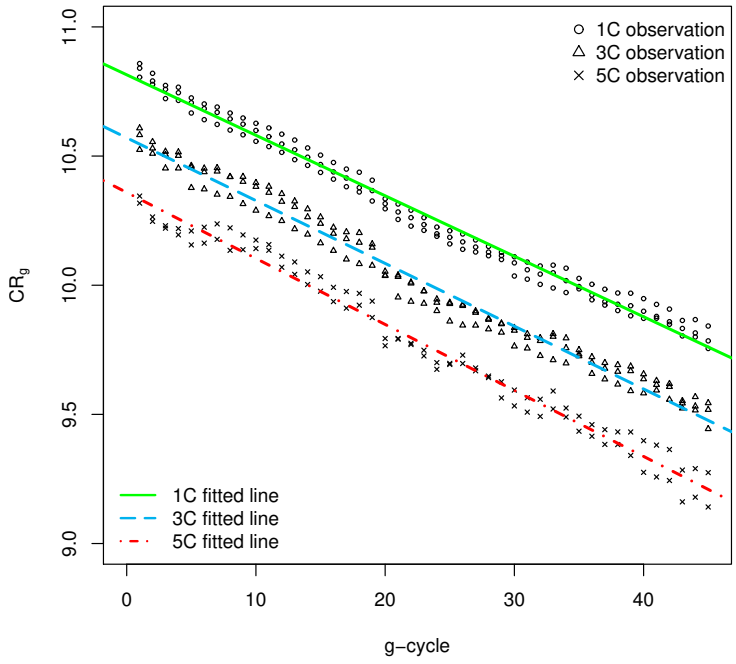

Figure 2: The CR_g plots of 8 samples over g-cycle time.

In the following, note that CR_g is a proportional function of cumulative total discrarge times in a g-cycle time. Hence, we use a recurrent approach to model the observed CR_g of

the battery dataset, illustrated in Figure 3. Here the CR_g are represented as the inter-arrival times of an artificial recurrent event process.

Since the inter-arrival times of events (CR_gs) are slightly decreasing over g-cycle times, the i.i.d. assumption of an RP inappropriate. To overcome the weakness of RP, Lindqvist *et al.* (2003) proposed the TRP model, in which the addition of a trend function enables one to model such a correlation structure. Therefore, in the next section, we will apply TRP model to fit the rechargeable battery dataset. The "time-scale" of this process will hence be the CR_g-scale, and we shall let Z_i denote the i^{th} observed CR_g, which is now the inter-arrival time of i^{th} event in T-process (before transformation).

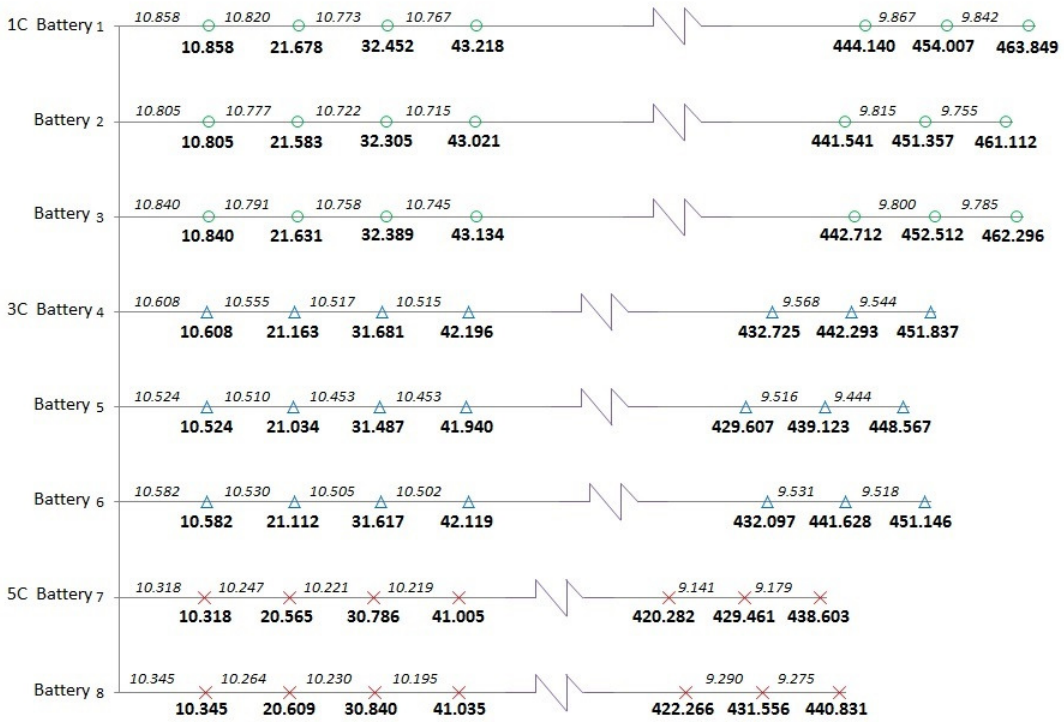

Figure 3: Recurrent event processes for the rechargeable battery dataset.

3 Preliminary Analysis

Given a specific discharge rate S, the TRP model can easily be introduced via Figure 4 (which is slightly modified from Lindqvist *et al.* (2003)), where T_i (Z_i) denotes the arrival (inter-arrival) time of i^{th} event in the original process (T-process) for $i = 1, 2, \cdots$, while $\Lambda(T_i)$ (X_i) denotes the arrival (inter-arrival) of i^{th} event in the transformed process ($\Lambda(T)$-process). Lindqvist *et al.* (2003) assumed that the inter-arrival time of transformed process ($\Lambda(T)$-process) will follow a sequence of i.i.d. random variables with distribution function F. In addition, to avoid non-identifiability issue, we require an additional condition that the mean of F is 1. That is, $X_i \overset{i.i.d.}{\sim} F$, where $E(X_i) = 1$ and $X_i = \Lambda(T_i) - \Lambda(T_{i-1})$, $i = 1, 2, \cdots$. Furthermore, if there exists $\lambda(t)$ such that $\Lambda(t) = \int_0^t \lambda(u)du$, then the T-process $T_1, T_2, \ldots$ is denoted as TRP$(F, \lambda(t))$, and $\lambda(t)$ is called the trend function of TRP model.

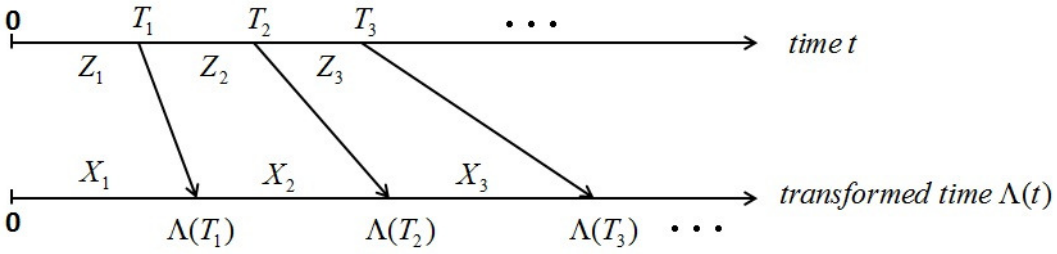

Figure 4: The illustration of the TRP.

For the trend function $\lambda(t)$, log-linear function (ae^{bt}) and power-law function (abt^{b-1}) are widely used in TRP model. In addition, log-normal, Weibull and normal distributions are widely used models for F. Therefore, under the restriction of mean 1, we adopted $F_1 = \text{LN}(-\alpha^2/2, \alpha^2)$, $F_2 = \text{Weib}(1/\Gamma((\beta)^{-1} + 1), \beta)$ and $F_3 = N(1, \sigma^2)$ in the following study, where α, β and σ are the logarithmic scale, shape and scale parameters of log-normal,

Weibull and normal distributions, respectively. Under these two trend functions and three distributions, we first calculate, using our data, the maximum log-likelihood for the model selections of 6 possible candidates under 3 different settings of stress, and Table 1 shows the results of maximum values of log-likelihood for all combinations. From Table 1, we find that the "log-linear" trend function has better performance than that of "power-law". In addition, log-normal and normal distributions outperform Weibull distribution in log-likelihood performances, while the log-likelihood performances of log-normal and normal distributions are compatible.

Table 1: Maximum log-likelihood for F and $\lambda(t)$ in TRP model.

distribution	power-law			log-linear		
	1C	3C	5C	1C	3C	5C
Weibull	91.50480	75.96159	38.95450	255.73305	228.97714	144.06864
log-normal	71.29970	59.90468	27.56702	264.84722	231.45690	144.79353
normal	72.14140	60.69355	28.17432	264.81415	231.49726	144.83904

Therefore, we then use the log-linear trend function to calculate ML estimates for a, b, α, β and σ of all 8 batteries and their corresponding maximum log-likelihood as shown in Table 2. Furthermore, the scatter plots of these estimates with respect to discharge rate are shown in Figure 5. Figure 5 shows that $\hat{a}$, $\hat{b}$, $\hat{\alpha}$, $\hat{\beta}$ and $\hat{\sigma}$ have very good linear relationship with stress S. In addition, from Table 2, all log-likelihood performances are very close and compatible. Considering the setting of accelerated testing, the mean and variance of the normal distribution are easier to implement than the two others. Therefore, in the following

study, we adopt the normal distribution for the renewal distribution and the relationships of $a(S)$, $b(S)$ and $\sigma(S)$ vis S can be reasonably modelled by

$$\begin{aligned} a(S) &= a_0 + a_1 S; \\ b(S) &= b_0 + b_1 S; \\ \sigma(S) &= c_0 + c_1 S. \end{aligned} \tag{1}$$

That is, considering higher stress S, TRP with discharge rate S can be denoted as accelerated testing version of TRP model and hereafter, we call it as ATRP$(F|S, \lambda(t|S))$. In addition, we adopt $F|S = N(1, \sigma^2(S))$ and $\lambda(t|S) = a(S)e^{b(S)t}$ in this study.

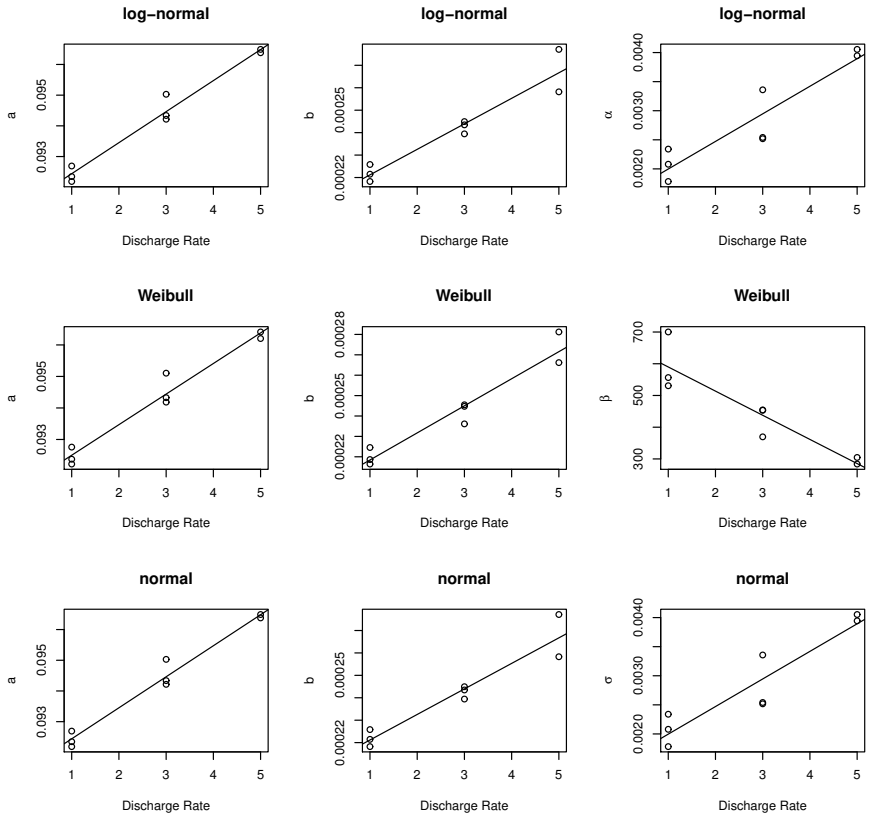

Figure 5: The scatter plot of $\hat{a}$, $\hat{b}$, $\hat{\alpha}$, $\hat{\beta}$ and $\hat{\sigma}$ versus S.

Table 2: ML estimates of a, b, α, β and σ in the preliminary analysis.

	Discharge Rate	Sample	$\hat{a}(*10^{-2})$	$\hat{b}(*10^{-4})$	$\hat{\alpha}(*10^{-3})$	log-likelihood
log-normal	1C	1	9.219	2.182	2.340	103.832
		2	9.269	2.215	2.080	109.405
		3	9.235	2.258	1.783	116.212
	3C	4	9.422	2.435	3.359	88.746
		5	9.503	2.394	2.519	102.032
		6	9.434	2.449	2.541	101.380
	5C	7	9.649	2.771	3.946	82.860
		8	9.638	2.582	4.054	81.399
	Discharge Rate	Sample	$\hat{a}(*10^{-2})$	$\hat{b}(*10^{-4})$	$\hat{\beta}(*10^{2})$	log-likelihood
Weibull	1C	1	9.222	2.164	5.565	107.050
		2	9.276	2.286	5.307	108.017
		3	9.237	2.245	7.002	118.609
	3C	4	9.418	2.447	3.696	90.719
		5	9.510	2.361	4.544	101.801
		6	9.433	2.455	4.533	101.117
	5C	7	9.641	2.812	2.839	82.143
		8	9.620	2.662	3.046	82.983
	Discharge Rate	Sample	$\hat{a}(*10^{-2})$	$\hat{b}(*10^{-4})$	$\hat{\sigma}(*10^{-3})$	log-likelihood
normal	1C	1	9.219	2.182	2.339	103.858
		2	9.269	2.215	2.080	109.405
		3	9.235	2.258	1.782	116.233
	3C	4	9.422	2.435	3.357	88.777
		5	9.503	2.394	2.518	102.044
		6	9.434	2.449	2.541	101.387
	5C	7	9.649	2.771	3.944	82.875
		8	9.638	2.583	4.053	81.416

Remark **:** Lindqvist *et al.* (2003) and Lindqvist (2006) introduced heterogeneity into the TRP model, called HTRP, by using unobservable random variables to multiply the trend function. That is, the differences between sample performances are modeled by assuming that the trend function $\lambda(\cdot)$ vary from sample to sample. The results in Table 2 demonstrate that the variation of $\hat{a}$ within each discharge rate are very small. From this observation, the

effect of heterogeneity will be ignored in this study.

4 Problem Formulation and its Statistical Inference

Suppose that normal use discharge rate is S_0 and ω is a known threshold. Under S_0, suppose the observed events $t_1, t_2, \ldots$ follow ATRP$(F|S_0, \lambda(t|S_0))$, and let Z_i denote the inter-arrival time of i^{th} event in T-process, where $F|S_0 = N(1, \sigma^2(S_0))$, $\lambda(t|S_0) = a(S_0)e^{b(S_0)t}$, and $a(\cdot)$, $b(\cdot)$ and $\sigma(\cdot)$ are given in Eq.(1). Then a random variable Y can be defined as time-to-failure of battery if

$$Y = \inf\{i : Z_i \leq \omega\}.$$

The goal of this study is to estimate the EOP which is the expected value of time-to-failure distribution and is given by EOP $= \mathrm{E}(Y)$. However, it is not easy to find the exact distribution of Y. Therefore, in this study, we slightly modify the definition of EOP as follows:

$$\text{EOP} = \inf\{i : \mathrm{E}(Z_i) \leq \omega\}. \tag{2}$$

Note that the EOP of a highly-reliable rechargeable battery may be very large. Therefore, in the following, an accelerated testing procedure is adopted to shorten the life testing time.

Suppose that $(S_0 <) S_1 < \cdots < S_K$ denote K increasingly high discharge rates, and there are n_k samples tested under stress S_k. Therefore, we assume that the events $T_{1jk}, T_{2jk}, \ldots, T_{m_{jk}jk}$ (obtained from the j^{th} sample under stress S_k) follow ATRP$(F|S_k, \lambda(t|S_k))$, where $j = 1, \cdots, n_k$, $k = 1, \cdots, K$, and m_{jk} is denoted as the total number of events in this

situation. Based on Section 3, we take $F|S_k = N(1, \sigma^2(S_k))$ and $\lambda(t|S_k) = a(S_k)e^{b(S_k)t}$, where the relations of $a(\cdot)$, $b(\cdot)$ and $\sigma(\cdot)$ are given in Eq.(1). Let Z_{ijk} be the inter-arrival time of the i^{th} events in T-process $T_{1jk}, T_{2jk}, \ldots$ with $Z_{ijk} = T_{ijk} - T_{i-1,jk}$. Figure 6 illustrates the formulations for clarity.

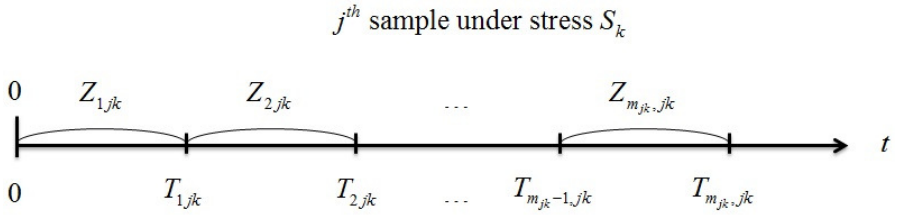

Figure 6: The TRP formulation for the battery recurrent data.

4.1 Goal of This Study

Now, based on the observed data in the above-mentioned accelerated testing, $\{Z_{ijk}\}$, $1 \le i \le m_{jk}$, $1 \le j \le n_k$, and $1 \le k \le K$, we will provide a systematic approach to make inference of the EOP of rechargeable battery. Some typical decision problems are as follows:

(1) how can we estimate the unknown parameters $\boldsymbol{\theta} = (a_0, a_1, b_0, b_1, c_0, c_1)$?

(2) how can we predict the EOP under S_0?

(3) how can we obtain the confidence interval of $\boldsymbol{\theta}$ and EOP?

In the following, we will address these decision problems in sequence.

4.2 Point Estimation for $\boldsymbol{\theta}$

For a fixed S_k ($k = 1, \ldots, K$), suppose that the j^{th} sample has observations at $\boldsymbol{t_{jk}} = (t_{1jk}, t_{2jk}, \ldots, t_{m_{jk},j,k})$ and follows ATRP$(F|S_k, \lambda(t|S_k))$. Based on the expression of (6) in Lindqvist *et al.*(2003) (last part can be ignored in this study), the corresponding likelihood function is given by

$$\prod_{i=1}^{m_{jk}} f\Big(\Lambda(t_{ijk}|S_k;\boldsymbol{\theta}) - \Lambda(t_{i-1,jk}|S_k;\boldsymbol{\theta})|S_k;\boldsymbol{\theta}\Big) \times \lambda(t_{ijk}|S_k;\boldsymbol{\theta}),$$

where f is the density function corresponding to $N(1, \sigma^2(S_k))$ and $\lambda(t|S_k) = a(S_k)e^{b(S_k)t}$. Suppose that the i.i.d. assumption holds among n_k samples. Then the likelihood function given data $\boldsymbol{t_k} = (\boldsymbol{t_{1k}}, \ldots, \boldsymbol{t_{n_k k}})$ can be expressed as

$$L(\boldsymbol{\theta}|\boldsymbol{t_k}; S_k) = \prod_{j=1}^{n_k} \left(\prod_{i=1}^{m_{jk}} f\Big(\Lambda(t_{ijk}|S_k;\boldsymbol{\theta}) - \Lambda(t_{i-1,jk}|S_k;\boldsymbol{\theta})|S_k;\boldsymbol{\theta}\Big) \times \lambda(t_{ijk}|S_k;\boldsymbol{\theta}) \right).$$

Hence, the total likelihood function of $\boldsymbol{\theta}$ for the proposed ATRP model can be expressed as

$$L(\boldsymbol{\theta}) = \prod_{k=1}^{K} L(\boldsymbol{\theta}|\boldsymbol{t_k}; S_k). \tag{3}$$

By using the built-in R function optim() to maximize Eq.(3), the maximum likelihood estimation (MLE) for unknown parameters $\boldsymbol{\theta}$ can be directly obtained to be $\hat{\boldsymbol{\theta}} = (\hat{a}_0, \hat{a}_1, \hat{b}_0, \hat{b}_1, \hat{c}_0, \hat{c}_1)$.

4.3 Point Estimation for EOP

Under S_0, we have $\lambda(t|S_0) = a(S_0)e^{b(S_0)t}$, and $\Lambda(t|S_0) = \frac{a(S_0)}{b(S_0)}(e^{b(S_0)t} - 1)$. Let X_{l0} denote the l^{th} inter-arrival time of $\Lambda(T)$-process under S_0. That is, X_{l0} follows i.i.d. $N(1, \sigma^2(S_0))$.

Therefore, the c.d.f. of T_i (the i^{th} arrival time of T-process under S_0) can be obtained by

$$\begin{aligned} F_{T_i}(t) &= P(T_i \le t) = P(\Lambda(T_i|S_0) \le \Lambda(t|S_0)) \\ &= P\left(\frac{\Lambda(T_i|S_0) - i}{\sqrt{i\sigma^2(S_0)}} \le \frac{\Lambda(t|S_0) - i}{\sqrt{i\sigma^2(S_0)}}\right) = \Phi\left(\frac{\Lambda(t|S_0) - i}{\sqrt{i\sigma^2(S_0)}}\right), \end{aligned}$$

due to the fact of $\Lambda(T_i|S_0) = \sum_{l=1}^{i} X_{l0} \sim N(i, i\sigma^2(S_0))$. Moreover, the p.d.f. of T_i can be given by

$$f_{T_i}(t) = \frac{d}{dt} F_{T_i}(t) = \phi\left(\frac{\Lambda(t|S_0) - i}{\sqrt{i\sigma^2(S_0)}}\right) \frac{\lambda(t|S_0)}{\sqrt{i\sigma^2(S_0)}},$$

where $\phi(\cdot)$ is p.d.f. of the standardized normal. However, it is not easy to obtain the expectation of T_i directly. Therefore, we then consider the approximation of Taylor expansion for $\mathrm{E}(T_i)$. First, because T_i can be expressed as

$$T_i = \Lambda^{-1}\left(\sum_{l=1}^{i} X_{l0}|S_0\right) = \frac{1}{b(S_0)} \log\left(1 + \frac{b(S_0)}{a(S_0)} \sum_{l=1}^{i} X_{l0}\right),$$

set $Y_i = 1 + \frac{b(S_0)}{a(S_0)}\left(\sum_{l=1}^{i} X_{l0}\right)$, then $\mathrm{E}(Y_i) = \mu_Y = 1 + i * \frac{b(S_0)}{a(S_0)}$ and $\mathrm{Var}(Y_i) = i * \sigma^2(S_0) * (\frac{b(S_0)}{a(S_0)})^2$. We can approximate $\log Y_i$ by Taylor expansion about μ_Y and we have the following result:

$$T_i = \frac{1}{b(S_0)} \log Y_i \approx \frac{1}{b(S_0)}\left(\ln \mu_Y + \frac{(Y_i - \mu_Y)}{\mu_Y} - \frac{(Y_i - \mu_Y)^2}{2\mu_Y^2}\right).$$

Therefore, we have the expectation of T_i given $\boldsymbol{\theta}$

$$\begin{aligned} \mathrm{E}(T_i|\boldsymbol{\theta}) &\approx \frac{1}{b(S_0)}\left(\ln \mu_Y - \frac{\mathrm{Var}(Y_i)}{2\mu_Y^2}\right) \\ &\approx \frac{1}{b(S_0)}\left(\log\left(1 + \frac{i * b(S_0)}{a(S_0)}\right) - \frac{i * \sigma^2(S_0)}{2(i + a(S_0)/b(S_0))^2}\right), \end{aligned}$$

and

$$\begin{aligned} \mathrm{E}(Z_i|\boldsymbol{\theta}) &= \mathrm{E}(T_i|\boldsymbol{\theta}) - \mathrm{E}(T_{i-1}|\boldsymbol{\theta}) \\ &\approx \frac{1}{b(S_0)}\left(\log\left(\frac{i + \frac{a(S_0)}{b(S_0)}}{(i-1) + \frac{a(S_0)}{b(S_0)}}\right) + \frac{\sigma^2(S_0)}{2}\left(\frac{i-1}{(i-1+\frac{a(S_0)}{b(S_0)})^2} - \frac{i}{(i+\frac{a(S_0)}{b(S_0)})^2}\right)\right). \quad (4) \end{aligned}$$

Now, let $\hat{a}(S_0)$, $\hat{b}(S_0)$ and $\hat{\sigma}(S_0)$ denote the MLEs of $a(S_0)$, $b(S_0)$ and $\sigma(S_0)$, respectively, in Section 4.2. By plugging MLEs $\hat{\boldsymbol{\theta}}$ into Eq.(4), the estimation of EOP can be expressed as follows:

$$\widehat{\mathrm{EOP}}(\omega) = \inf\{i : \mathrm{E}(Z_i|\hat{\boldsymbol{\theta}}) \leq \omega\}. \tag{5}$$

4.4 Confidence Intervals for $\boldsymbol{\theta}$ and EOP

We adopt the parametric bootstrap method (Efron, 1979) to estimate standard errors of the MLEs and to obtain $100(1-\alpha)\%$ approximate confidence intervals for EOP and each parameter. For the parametric bootstrap method, first we use the definition of the TRP model to generate bootstrap samples from the estimated model using $\hat{\boldsymbol{\theta}}$. The confidence intervals based on the parametric bootstrap method can be described as follows:

1. Set $r = 1$.
2. Simulate a dataset with stresses $S_1, S_2, \ldots, S_K$, denoted $\boldsymbol{D}^{(r)} = \{t_{ijk}^{(r)} : 1 \leq i \leq m_{jk}, 1 \leq j \leq n_k, 1 \leq k \leq K\}$, from estimates $\hat{\boldsymbol{\theta}}$, respectively.
3. Compute the estimates $\tilde{\boldsymbol{\theta}}^{(r)}$ from $\boldsymbol{D}^{(r)}$ by Eq.(3).
4. Calculate the EOP estimation $\widetilde{\mathrm{EOP}}^{(r)}$ by Eq.(5).
5. Repeat steps 2-4 R times to obtain $\tilde{\boldsymbol{\theta}} = \{\tilde{\boldsymbol{\theta}}^{(r)}; r = 1, \cdots, R\}$ and $\widetilde{\mathrm{EOP}} = \{\widetilde{\mathrm{EOP}}^{(r)}; r = 1, \cdots, R\}$

The standard errors for the $\hat{\boldsymbol{\theta}}$ and $\widehat{\mathrm{EOP}}$ are estimated by bootstrap sample standard deviation. Thus, the corresponding $100(1-\alpha)\%$ approximate confidence intervals are the $\alpha/2$ and $(1-\alpha/2)$ quantiles of ordered $\tilde{\boldsymbol{\theta}}$ and $\widetilde{\mathrm{EOP}}$.

5 Rechargeable Battery Data Revisited

In practice, the EOP of battery is usually set as the cycle time when CR is reduced to 80%. Thus, the threshold value for g-cycle times is $\omega = 8$ in our study. To revisit the rechargeable battery dataset, we have $K = 3$, $(n_1, n_2, n_3) = (3, 3, 2)$ and $m_{jk} = 45$, for all j, k. By adopting the proposed ATRP model, the point estimates and 95% confidence intervals for $\boldsymbol{\theta}$ and EOP (with $R = 1000$ bootstrap samples) are as shown in Table 3. The results of the 95% CIs for a_1, b_1 and c_1 support that we necessarily consider the effect of accelerated testing in the TRP model. Furthermore, reconsidering the discard of first 7 g-cycle times, the final estimate of EOP, denoted by EOP_0, is 161 (=154+7) g-cycle times, and its corresponding 95% CI is [159,164]. Note that the bootstrap approach for constructing 95% CI in this study is quite similar to that of the conventional MLE approach:[161±1.96*1.54]=[158,164].

Table 3: MLEs, standard errors and 95% confidence intervals for $\boldsymbol{\theta}$ and EOP.

Parameter	MLE	SE	95% CI
a_0	9.14×10^{-2}	7.05×10^{-5}	$[9.13\times10^{-2},9.16\times10^{-2}]$
a_1	1.02×10^{-3}	2.65×10^{-5}	$[9.60\times10^{-4},1.06\times10^{-3}]$
b_0	2.10×10^{-4}	2.87×10^{-6}	$[2.04\times10^{-4},2.16\times10^{-4}]$
b_1	1.12×10^{-5}	1.08×10^{-6}	$[9.30\times10^{-6},1.34\times10^{-5}]$
c_0	2.92×10^{-3}	2.76×10^{-4}	$[2.35\times10^{-3},3.42\times10^{-3}]$
c_1	4.42×10^{-4}	1.03×10^{-4}	$[2.36\times10^{-4},6.42\times10^{-4}]$
EOP	154	1.54	[152,157]
EOP_0	161	1.54	[159,164]

5.1 Model Checking and Residual Analysis

First, we use the residual plots to detect the model fit. Let residuals be $(t_{ijk} - \hat{t}_{i,k})$, where $\hat{t}_{i,k}$ is the estimate of i^{th} events under stress S_k. Thus, we plot the residuals against g-cycle times for each discharge rate, respectively, as shown in Figure 7. The results demonstrate that there is no clear inappropriate pattern.

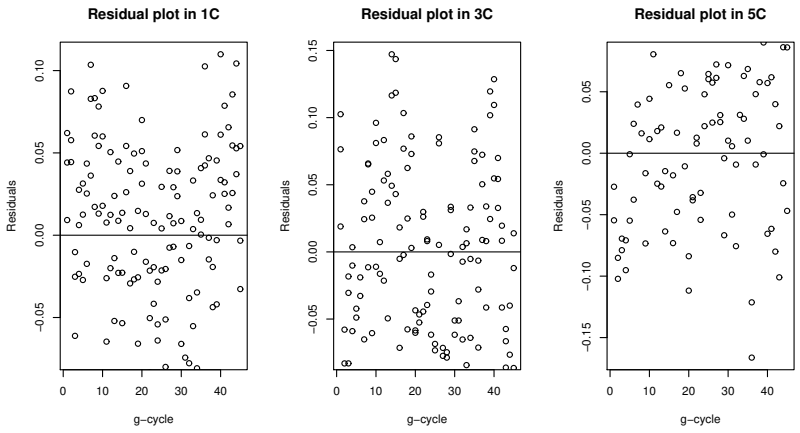

Figure 7: The residual plots for ATRP models.

Moreover, we need to check whether the inter-arrival times of the transformed process will follow i.i.d. assumption for all $\{S_k\}_{k=1}^3$. That is, $\hat{X}_{ijk} = \hat{\Lambda}(t_{i,j,k}) - \hat{\Lambda}(t_{i-1,j,k}) \overset{i.i.d}{\sim} N(1, \hat{\sigma}^2(S_k))$. We first apply Q-Q plots and the Kolmogorov-Smirnov (K-S) test to check the "normality assumption" for all $\{S_k\}_{k=1}^3$, and the results are shown in Figure 8 and Table 4, respectively. Note that all the fitted curves are close to the expected diagonal line and the p-values of K-S test support that the normal distribution can be reasonably used to characterize the underlying distribution of inter-arrival times of the transformed process. Furthermore, the Mann-Kendall (M-K) rank test is used to the "independence" and the results are shown in Table 4. Note that all p-values in Table 4, except one, are larger than 0.1 and hence there is

not no strong evidence to reject the "independence" of the inter-arrival of the transformed-process in the proposed ATRP model.

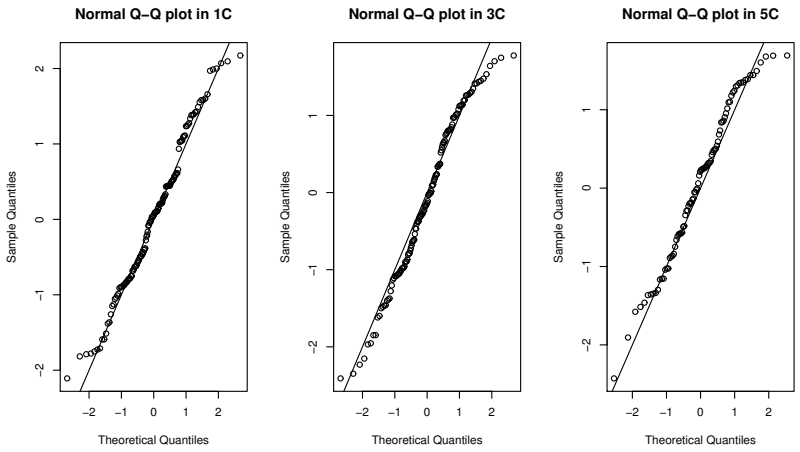

Figure 8: Q-Q plots for ATRP models.

Table 4: P-values for Kolmogorov-Smirnov (K-S) test and Mann-Kendall (M-K) rank test.

	1C			3C			5C	
	B1	B2	B3	B4	B5	B6	B7	B8
K-S test	0.6705			0.3362			0.3831	
M-K rank test	0.1003	0.6956	0.1044	0.6387	0.2998	0.8602	0.0199	0.1423

5.2 Simulation Study of the Effects of n and m

EOP prediction of the proposed ATRP model may depend on the number of testing batteries and testing g-cycle times. Therefore, we also conducted a simulation study to illustrate the performance of the ATRP model under various combinations of sample size n and number m of g-cycle times. For illustrative purposes, in the following, we treat the estimates in Table 3 as the true process parameters of ATRP model. Under the specific combinations of (n,

$m)$, $n = 1, \ldots, 5$, $m = 10, 20, \ldots, 50$, we first generated 1C, 3C and 5C accelerated battery data and use the proposed ATRP model to predict the 0.5C EOP. With 1000 simulations, the average of 0.5C EOP prediction, $\widehat{\text{EOP}}(n, m)$, can be obtained directly and a relative bias (RB) is defined as follows:

$$\widehat{\text{RB}}(n, m) = \frac{\widehat{\text{EOP}}(n, m) - \text{EOP}}{\text{EOP}} \times 100\%,$$

where EOP=153.4837 is the true EOP value based on 10000 simulations from the proposed ATRP model with the parameter settings shown in Table 3. This index can be used to measure the accuracy of EOP prediction and the results are shown in Table 5. We found that all RBs are very small, except for the cases of $(n, m) = (1, 10)$ or $(n, m) = (2, 10)$. Specifically, the RB will be less than 0.82% with $m \geq 20$ and $n \geq 2$ in this study. It means that letting each stress level have two testing batteries and each battery have 200 testing cycle times will be a good strategy for arranging a 3-level accelerated battery experiment if we want to control the RB to be less than 0.82%.

Table 5: The relative biases ($\widehat{\text{RB}}(n, m)$) for EOP.

$n \setminus m$	10	20	30	40	50
1	4.83%	1.10%	0.69%	0.56%	0.64%
2	2.28%	0.82%	0.65%	0.56%	0.58%
3	1.80%	0.75%	0.57%	0.54%	0.57%
4	1.32%	0.71%	0.68%	0.57%	0.52%
5	1.31%	0.57%	0.53%	0.55%	0.53%

6 Justification and Comparison of EOP Performance

In the following, we use two examples to address the prediction performance of the proposed ATRP procedure with that of other competing models. Specifically, we will compare the EOP prediction of battery dataset by the proposed ATRP model and linear regression model with time series errors in Sections 6.1 and 6.2. In addition, the NASA battery dataset in Sections 6.3 is used to compare the prediction performance of the proposed model with other competing models proposeed by Ng *et al.* (2014), Xu *et al.* (2016) and Cheng *et al.* (2015).

6.1 Model Fitting of Battery Data by Regression Model with Time Series Errors and the ATRP Model

The observed CR_g in the battery dataset is a sequence of time series data. Therefore, a linear regression model with time series errors (LRWTSE, Tsay, 1984) is a potential model to analyze this dataset. The LRWTSE model can be written as follow:

$$y_t = \beta_0 + \beta_1 t + \epsilon_t,$$

where ϵ_t follows an ARMA(p,q) model. That is, $\epsilon_t - \phi_1\epsilon_{t-1} - \cdots - \phi_p\epsilon_{t-p} = z_t - \theta_1 z_{t-1} - \cdots - \theta_q z_{t-q}$, where $z_t \overset{i.i.d.}{\sim} N(0, \sigma_0^2)$. We found that all battery data are well fitted by the linear regression model with AR(1) error and the results are shown in Table 6, where $\hat{\beta}_0$, $\hat{\beta}_1$, $\hat{\phi}$ and $\hat{\sigma}_0^2$ are the estimates of the parameters, respectively. By using one-step-ahead forecasting, we obtained the predictions of CR_g for all batteries and the results are shown in the left hand side (LHS) of Figure 9. For example, the 30^{th} g-cycle CR_g predictions for 8 batteries (B1∼B8) are (10.14, 10.08, 10.11, 9.87, 9.80, 9.86, 9.56, 9.63). Therefore, by adopting the

linear relationship between CR_g predictions and discharge rate, the 0.5C 30^{th} g-cycle CR_g prediction is 10.17 which can be obtained via extrapolation and the results are shown in right hand side (RHS) of Figure 9. Hence, i^{th} g-cycle CR_g prediction under 0.5C can be obtained directly, for all $i = 1, 2, \ldots$.

Table 6: The estimates of parameters in the linear regression model with AR(1) error.

Battery	$\hat{\beta}_0$	$\hat{\beta}_1$	$\hat{\phi}$	$\hat{\sigma}_0^2$
B1	10.7511	-0.0205	0.9062	1.5×10^{-4}
B2	10.7515	-0.0223	0.7971	2.2×10^{-4}
B3	10.7754	-0.0223	0.8475	1.4×10^{-4}
B4	10.5746	-0.0234	0.8233	4.7×10^{-4}
B5	10.5047	-0.0235	0.6793	4.6×10^{-4}
B6	10.5793	-0.0241	0.7432	3.9×10^{-4}
B7	10.3555	-0.0265	0.5400	8.0×10^{-4}
B8	10.3600	-0.0245	0.7540	7.3×10^{-4}

Generally speaking, the battery data in this study are not able to justify the quality of the EOP prediction at 80%. The main reason is that our battery data did not collect enough CR observations that truly crossed the given threshold 80%. As mentioned in Section 2, for the purpose of model validation, this battery experiment also provided the CR values of two batteries under normal use condition 0.5C. After taking the summation of 10 capacity ratios, their CR_g values are around 9.9 at the end of 45 g-cycle testing times. Therefore, we adopt the training data with 30 and 35 g-cycle times of 1C, 3C and 5C to predict the CR_g values in 0.5C with $\omega = 9.9$. Figure 10 shows the 0.5C predicted curves from ATRP model and LRWTSE model. The corresponding sum of square errors (SSEs) of these two prediction

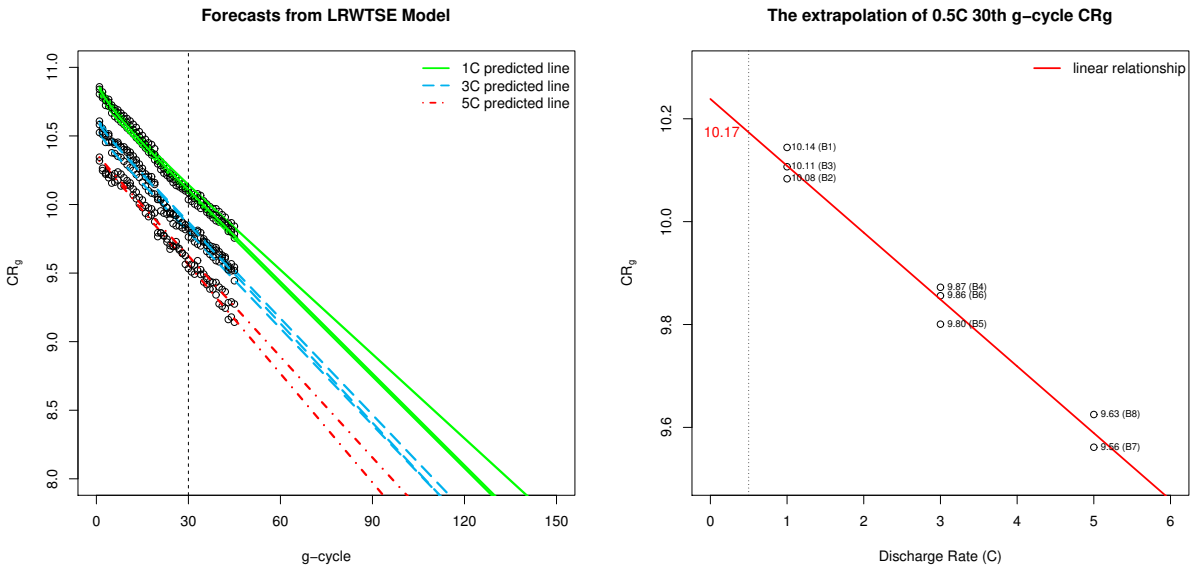

Figure 9: Forecasts and prediction from LRWTSE model.

models are also shown in Table 7. The results demonstrate that both models provide well fittings in the training data with 30 and 35 g-cycles. However, the SSE of the proposed ATRP model is much smaller than that of the LRWTSE model.

Table 7: SSEs of ATRP and LRWTSE models under the training data with 30 and 35 g-cycle times.

training data		ATRP	LRWTSE
Sample 1	30	0.0196	0.0605
	35	0.0068	0.0102
Sample 2	30	0.0214	0.0711
	35	0.0070	0.0105

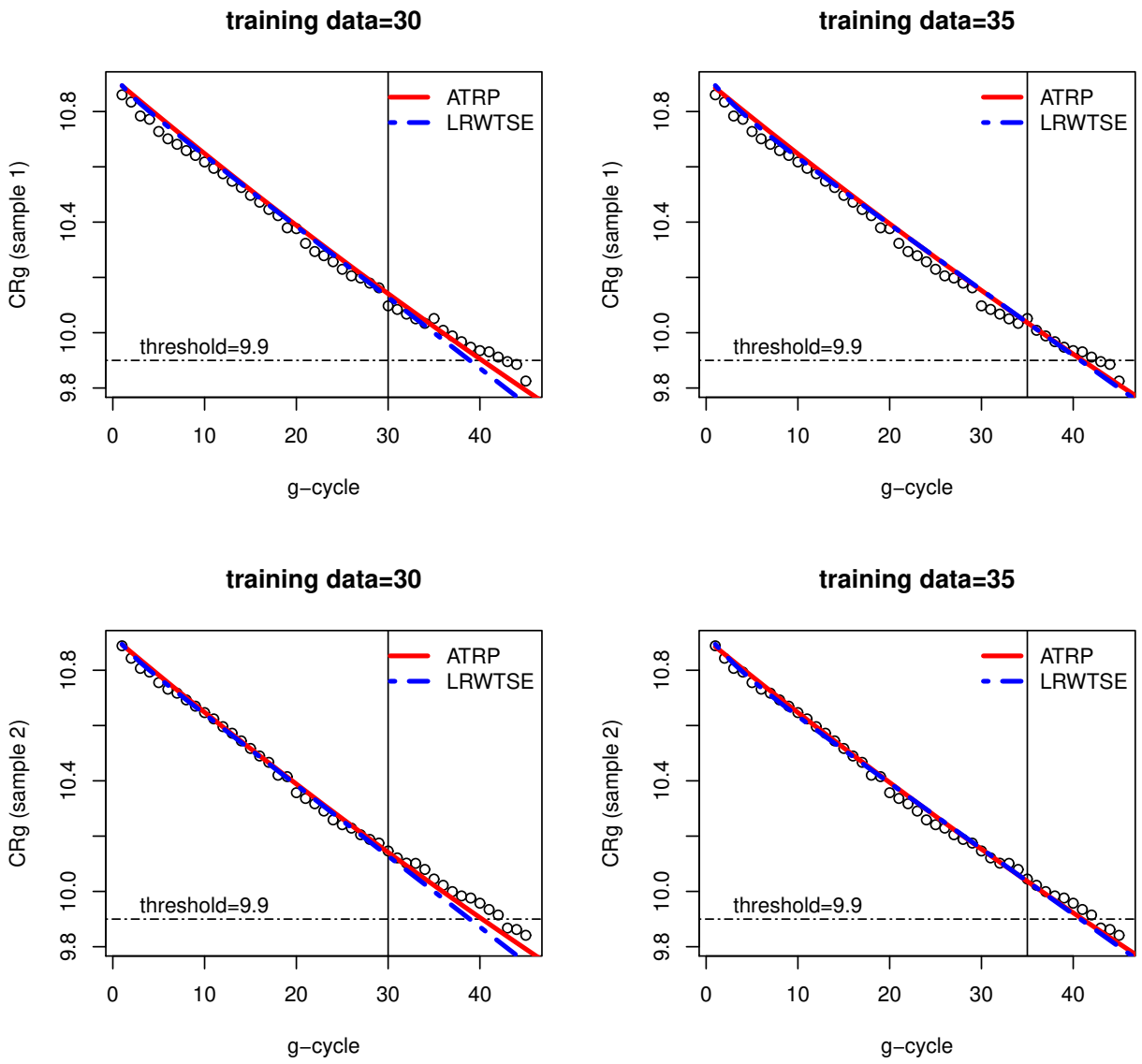

Figure 10: Justification of CR_g predictions from ATRP and LRWTSE models in 0.5C.

6.2 Comparison of EOP Predictions Between the ATRP and LRWTSE Models

By using 0.5C real data (stated in Section 6.1) for the purpose of model validation, Figure 11 shows the performance comparisons of our ATRP prediction with that of LRWTSE model.

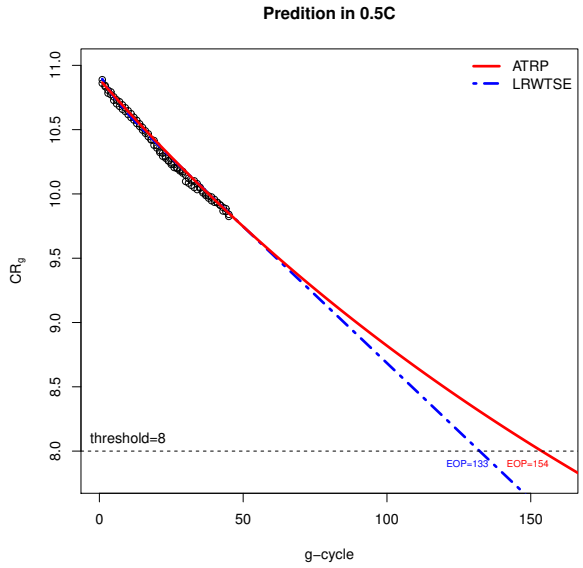

Figure 11: Predictions of ATRP and LRWTSE models in 0.5C.

It indicates that the short-term prediction makes no difference between both prediction curves. However, in the long-term prediction, LRWTSE is very similar to the case of a linear regression (with white noise) model, while the prediction by the ATRP model demonstrates a convex curve. The reason can be briefly stated as follow. Note that Eq.(4) can be approximately reduced to:

$$\mathrm{E}(Z_i|\hat{\boldsymbol{\theta}}) \approx \frac{1}{\hat{b}(S_0)} \left(\log \left(\frac{i + \frac{\hat{a}(S_0)}{\hat{b}(S_0)}}{(i-1) + \frac{\hat{a}(S_0)}{\hat{b}(S_0)}} \right) \right), \tag{6}$$

since $\hat{\sigma}^2(S_0) \approx 10^{-8}$. In addition, it is easy to see that $\frac{d^2}{d\ i^2}\mathrm{E}(Z_i|\hat{\boldsymbol{\theta}}) > 0$ for all i. Therefore, the convexity of $\mathrm{E}(Z_i|\hat{\boldsymbol{\theta}})$ follows directly. Hence, the time-dependent structure can be suitably captured by our proposed model. On the other hand, the EOP prediction by LRWTSE will be approximately underestimated about 13.6%.

6.3 EOP Performance Comparisons By Using NASA Dataset

The NASA battery dataset was collected by NASA Ames Prognostics Center of Excellence. This dataset has been widely used in Ng *et al.* (2014), Xu *et al.* (2016) and Cheng *et al.* (2015). We choose the batteries "B0005" and "B0006" (both batteries have 138 observations) to illustrate the performance of our proposed model. The main reason for choosing these two datasets is due to the fact that these batteries are tested under the same operating conditions (with temperatures (24°C) and discharge rate (2A)). Furthermore, their degradation paths have crossed the threshold (say 1.3 Ahr) and it allows us to have their true lifetime information.

Note that these two datasets did not have an accelerating variable, therefore, we only use TRP model (non-accelerated version of ATRP, M1) to address the prediction performances, in comparing with the following well-known models:

M2: exponential model (He *et al.* , 2011): $C_i = \alpha_0 e^{\alpha_1 i} + \alpha_2 e^{\alpha_3 i}$,

M3: second-order polynomial model (Micea *et al.* , 2011): $C_i = \alpha_0 + \alpha_1 i + \alpha_2 i^2$,

M4: exponential and polynomial model (Xing *et al.* , 2013): $C_i = \alpha_0 + \alpha_1 i^2 + \alpha_2 e^{\alpha_3 i}$,

M5: simple linear regression model (LM): $C_i = \alpha_0 + \alpha_1 i$,

where C_i denotes the observed capacity of i^{th} cycle in NASA dataset and all coefficients $\{\alpha_i\}_{i=1}^3$ are unknown. The comparisons of prediction performance of these 4 models together with TRP model are shown in Figure 12.

Note that the vertical (dotted) lines in the plots denote two different settings for the training data with 90 and 110 cycles (previous 90 or 110 cycles among 138 cycles); while the horizontal line at 1.3 denotes the threshold of the capacity. From the plots of battery

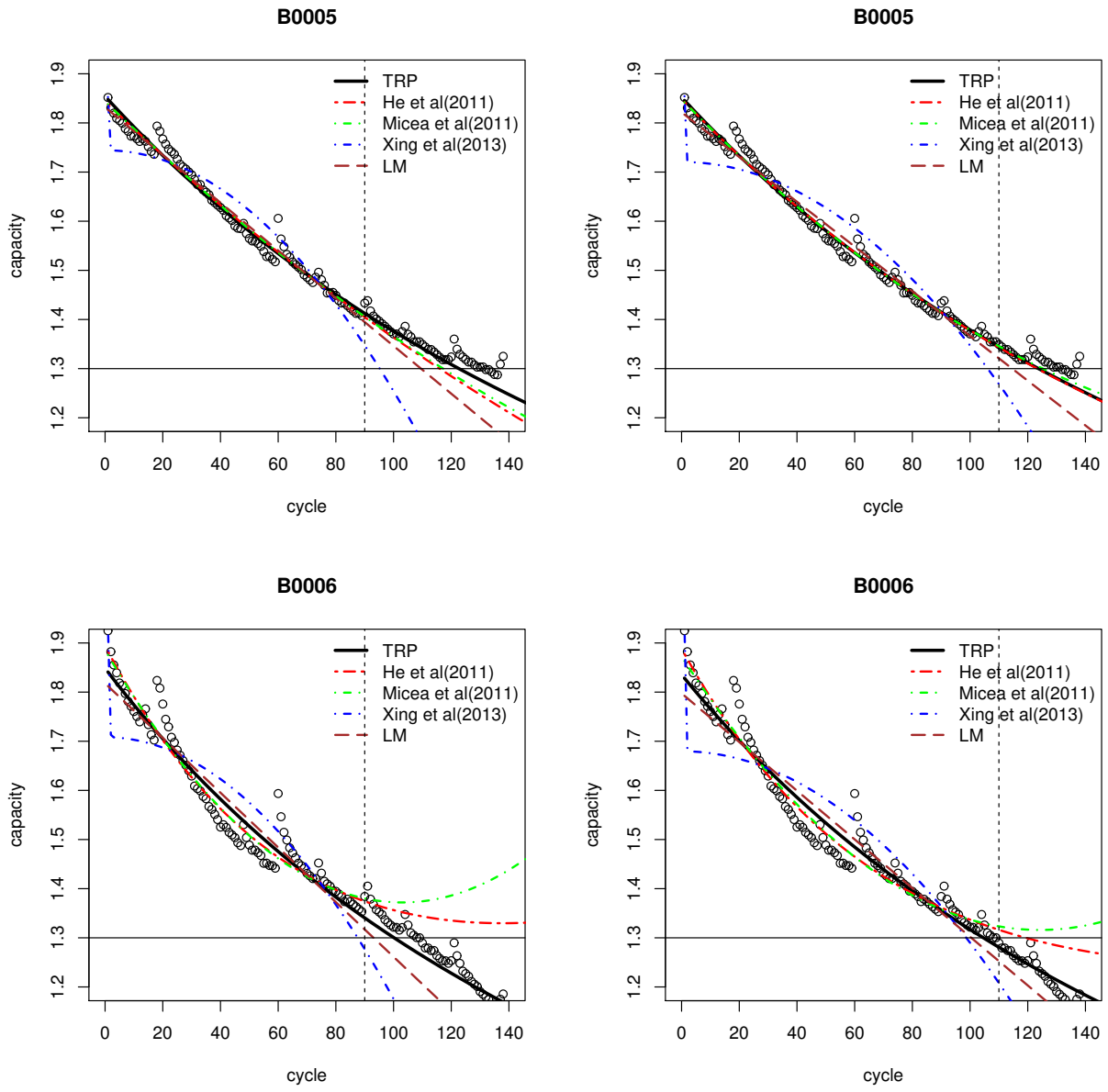

Figure 12: Comparisons of EOP prediction with observations 90 and 110.

"B0005", no matter 90 or 110 cycles is used, the prediction performance of TRP model is better than the other four models in the EOP prediction. For the case of battery "B0006", comparing with TRP model, it seems the EOP prediction of the other 4 models are very bad and the main reason may be due to the fact that all these regression models did not take

auto-correlated structure of the process into consideration. Furthermore, the root-mean-square errors (RMSEs) for all models are given to measure the prediction performance and the results are shown in Table 8. We found that the RMSE of M1 has the smallest RMSE, except for the case of RMSE_{110} at M3. The results are consistent with the plots shown in Figure 12. It means that our proposed model, in general, outperforms the existing methods in the EOP prediction.

Table 8: RMSEs for five candidate models under training data=90 and 110.

Battery	Root-mean-square error	Models				
		M1	M2	M3	M4	M5
B0005	RMSE_{90}	0.023	0.044	0.038	0.280	0.077
	RMSE_{110}	0.026	0.027	0.021	0.190	0.068
B0006	RMSE_{90}	0.029	0.090	0.142	0.291	0.092
	RMSE_{110}	0.020	0.075	0.102	0.158	0.047

*$\text{RMSE}_{90} = \sqrt{\sum_{i=91}^{138}(\hat{C}_i - C_i)^2/48}$ and $\text{RMSE}_{110} = \sqrt{\sum_{i=111}^{138}(\hat{C}_i - C_i)^2/28}$

7 Another Version of ATRP Model

Following the concept of Lindqvist *et al.* (2003), we always set the expectation of $F|S$ as 1 to avoid the non-identifiability issue of ATRP model. For example, we adopt $F|S = N(1, \sigma^2(S))$ in our study. However, based on the fundamental criterion of the accelerated testing, we may consider that the mean is usually a function of S, while keeping the standard deviation unchanged. That is, the new formulation for ATRP model has $F|S = N(\mu(S), 1)$ and $\lambda(t|S) = a^*(S)e^{b^*(S)t}$.

Similar to the preliminary analysis in Section 3, we need to check the relationships be-

tween model parameters $a^*(S)$, $b^*(S)$, $\mu(S)$ and stress S. Figure 13 supports that parameters $a^*(S)$, $b^*(S)$ still have good linear relationship with stress S, and $\mu(S)$ is recommended to have a log-linear relationship with S. Therefore, $a^*(S)$, $b^*(S)$ and $\mu(S)$ can be reasonably expressed as $a^*(S) = a_0^* + a_1^* S$; $b^*(S) = b_0^* + b_1^* S$; and $\log \mu(S) = c_0^* + c_1^* S$.

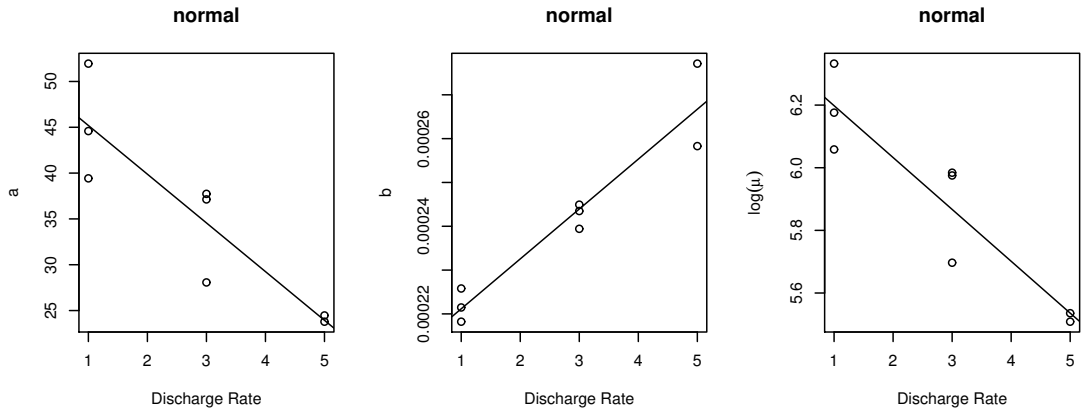

Figure 13: The scatter plot of $\hat{a}$, $\hat{b}$ and $\log \hat{\mu}$ versus S.

Table 9 summarizes a detailed comparisons of these two ATRP models. From Table 9, it is seen that the EOP predictions are the same for both models. It means that arranging the mean or the standard deviation as the function of testing stress did not have a significant effect on the EOP prediction. From the log-likelihood criterion, the LL of ATRP Model 1 is slightly larger than that of ATRP Model 2. However, from the viewpoint of acceleration, it seems that ATRP model 2 provides us a better explanation in practical applications.

8 Concluding Remarks

"How to obtain an accurate EOP prediction for rechargeable battery" is a great challenge to the manufacturers of information and communication technology industry. Traditionally,

Table 9: Summary of two ATRP models.

Model	ATRP Model 1	ATRP Model 2
$F\|S$	$N(1, \sigma^2(S))$	$N(\mu(S), 1)$
Stress relationship	$\sigma(S) = c_0 + c_1 S$	$\log \mu(S) = c_0^* + c_1^* S$
$\lambda(t\|S)$	$a(S)e^{b(S)t}$	$a^*(S)e^{b^*(S)t}$
Maximum log-likelihood	LL_1=639.95	LL_2=630.15
EOP Prediction	$\widehat{\text{EOP}}_1 = 154$	$\widehat{\text{EOP}}_2 = 154$
explanation	not easy to explain	easy to explain

regression prediction models (linear, second-order polynomial and exponential) are widely used in rechargeable battery datasets. However, these models are, in general, not capable of achieving better EOP prediction due to the fact that the time-dependent structure is not taken into consideration. In this article, based on a TRP model under the scenario of accelerated testing, we propose a novel approach to address this important problem. The advantage of our proposed ATRP model is that the auto-correlated structure can be appropriately characterized in comparing with the linear regression model with time series errors model (Tsay, 1984). Furthermore, the procedures of EOP prediction and its 95% CI are developed. Finally, we also use NASA battery dataset to compare the performance of EOP prediction with the existing methods, and the result shows that our proposed model is quite robust in EOP prediction.

At the end of this study, some concluding remarks are addressed as follows:

(a) We did not consider the heterogeneous TRP (HTRP) model due to the fact that the

unit-to-unit process variations are not significant. For practical applications, when the variations can not be ignored, the development of an accelerated testing version of HTRP model shall be an interesting topic for the future research.

(b) In this study, we only focus on a constant-stress accelerated degradation test for the purpose of the EOP lifetime prediction of rechargeable batteries. In real applications, however, the time-varying stress (or even cycle-testing) operational condition is very popular. Therefore, the modeling of a step-stress degradation path of dynamic discharge shall be an interesting and challenging issue for the future research.

References

BEBBINGTON, M.S. (2010). "Trends and clustering in the onsets of volcanic eruptions". *Journal of Geophysical Research: Solid Earth (1978-2012)*, **115.B1**.

CHENG, Y.; LU, C.; LI, T.; and TAO, L. (2015). "Residual lifetime prediction for lithium-ion battery based on functional principal component analysis and Bayesian approach". *Energy*, **90**, pp. 1983–1993.

COOK, R.J. and LAWLESS, J.F. (2007). *The statistical analysis of recurrent events*, Springer.

EFRON, B. (1979). "Bootstrap methods: another look at the jackknife". *The Annals of Statistics*, **7**, pp. 1–26.

FRANZ, J.; JOKIEL-ROKITA, A.; and MAGIERA, R. (2014). "Prediction in trend-renewal processes for repairable systems". *Statistics and Computing*, **24**, pp. 633–649.

GU, J.; BARKER, D.; and PECHT, M. (2007). "Prognostics implementation of electronics under vibration loading". *Microelectronics Reliability*, **47**, pp. 1849–1856.

HE, W.; WILLIARD, N.; OSTERMAN, M.; and PECHT, M. (2011). "Prognostics of lithium-ion batteries based on Dempster-Shafer theory and the Bayesian Monte Carlo method". *Journal of Power Sources*, **196**, pp. 10314–10321.

JOKIEL-ROKITA, A. AND MAGIERA, R. (2012). "Estimation of parameters for trend-renewal processes". *Statistics and Computing*, **22**, pp. 625–637.

LINDQVIST, B.H. (2006). "On the statistical modeling and analysis of repairable systems". *Statistical Science*, **21**, pp. 532–551.

LINDQVIST, B.H.; ELVEBAKK, G.; and HEGGLAND, K. (2003). "The trend-renewal process for statistical analysis of repairable systems". *Technometrics*, **45**, pp. 31–44.

LONG, B.; XIAN, W.; JIANG, L.; and LIU, Z. (2013). "An improved autoregressive model by particle swarm optimization for prognostics of lithium-ion batteries". *Microelectronics Reliability*, **53**, pp. 821–831.

LU, C.; TAO, L.; and FAN, H. (2014). "Li-ion battery capacity estimation: a geometrical approach". *Journal of Power Sources*, **261**, pp. 141–147.

MIAO, Q.; XIE, L.; CUI, H.; LIANG, W.; and PECHT, M. (2013). "Remaining useful life prediction of lithium-ion battery with unscented particle filter technique". *Microelectronics Reliability*, **53**, pp. 805–810.

MICEA, M.V.; UNGUREAN, L.; CARSTOIU, G.N.; and GROZA, V. (2011). "Online state-of-health assessment for battery management systems". *IEEE Transactions on Instrumentation and Measurement*, **60**, pp. 1997–2006.

NG, S.S.Y; XING, Y.; and TSUI, K.L. (2014). "A naive Bayes model for robust remaining useful life prediction of lithium-ion battery". *Applied Energy*, **118**, pp. 114–123.

PATTIPATI, B.; SANKAVARAM, C.; and PATTIPATI, K. (2011). "System identification and estimation framework for pivotal automotive battery management system characteristics". *IEEE Transactions on Systems, Man, and Cybernetics Part C: Applications and Reviews*, **41**, pp. 869–884.

PECHT, M. and DASGUPTA, A. (1995). "Physics-of-failure: an approach to reliable product development". *Journal of the Institute of Environmental Sciences*, **38**, pp. 30–34.

SPOTNITZ, R. (2003). "Simulation of capacity fade in lithium-ion batteries". *Journal of Power Sources*, **113**, pp. 72–80.

SAHA, B.; GOEBEL, K.; POLL, S.; and CHRISTOPHERSEN, J. (2007). "An integrated approach to battery health monitoring using Bayesian regression and state estimation". *IEEE Autotestcon*, pp. 646–653.

TSAY, R.S. (1984). "Regression Models with Time Series Errors". *Journal of the American Statistical Association*, **79**, pp. 118–124.

TANG, S.; YU, C.; WANG, X.; GUO, X.; and SI, X. (2014). "Remaining useful life prediction of lithium-ion batteries based on the Wiener process with measurement error". *Energies*, **7**, pp. 520–547.

XING, Y.; MA, E.W.M.; TSUI, K.L.; and PECHT, M. (2013), "An ensemble model for predicting the remaining useful performance of lithium-ion batteries". *Microelectronics Reliability*, **53**, pp. 811–820.

XU, X.; LI, Z.; and CHEN, N. (2016). "A hierarchical model for lithium-ion battery degra-

dation prediction". *IEEE Transactions on Reliability*, **65**, pp. 310–325.

ZHANG, J. and LEE, J. (2011). "A review on prognostics and health monitoring of Li-ion battery". *Journal of Power Sources*, **196**, pp. 6007-6014.